11–1

AGN Surveys and AGN Environment

11–2

Introduction

Result of previous lectures:

AGN produce large amounts of energy over timescales of $\gtrsim 10^8$ years and they strongly interact with their environment.

Questions:

- How do AGN form?
- What galaxies harbor AGN?
- Are these galaxies different from others?
- How do galaxies with AGN evolve? ("coevolution")

To answer these questions, we need to study statistical properties of AGN and their hosts, both among morphological type and with time: AGN surveys

11–3

Finding AGN, I

AGN surveys: searching for AGN.

Problem: AGN are rare objects

$\Longrightarrow$ need to detect them amongst much more numerous stars and galaxies

$\Longrightarrow$ need to find ways that quasars/AGN are "not stars"

Typical ways:

- measurement of SED
- emission line spectra
- variability

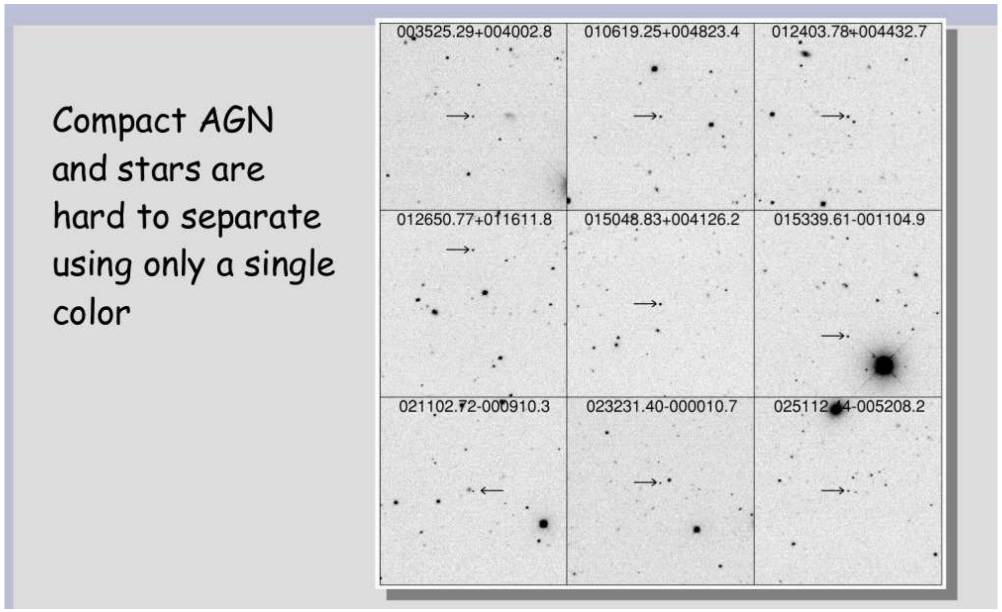

Koopmans, Lecture 10, Slide 09

Radio Surveys

Radio surveys: historically first way to find AGN

High success rate:

- Many radio sources are AGN
- very good positions
- very high sensitivity
- good sky coverage

Still: follow up observations are required.

But: Most AGN are not radio loud (90%!)

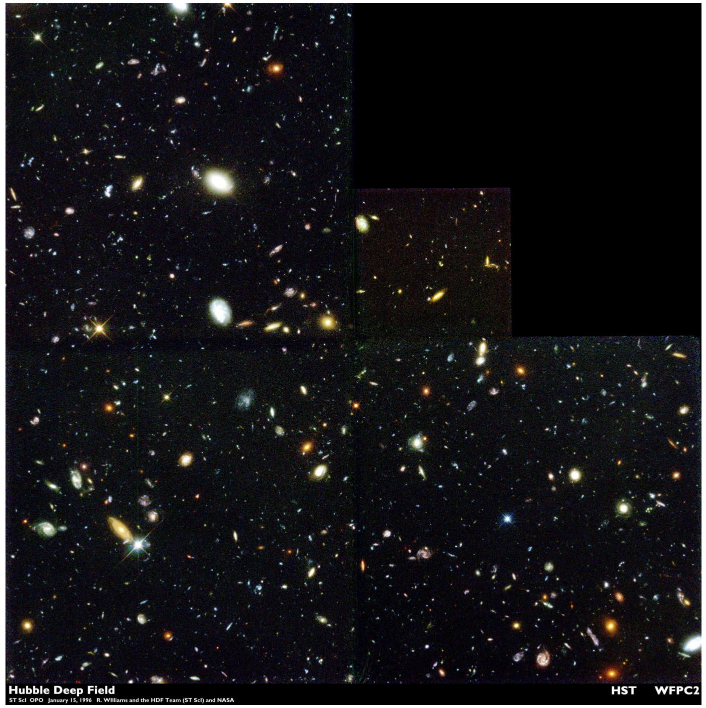

HDF: $\sim$ 150 ksec/Filter for 4 HST Filters made in 1995 December.
Many galaxies with weird shapes $\Longrightarrow$ protogalaxies!
Redshifts: $z \in [0.5, 5.3]$ (Fernández-Soto et al., 1999)

Hubble Deep Field, courtesy STScI

Optical Surveys

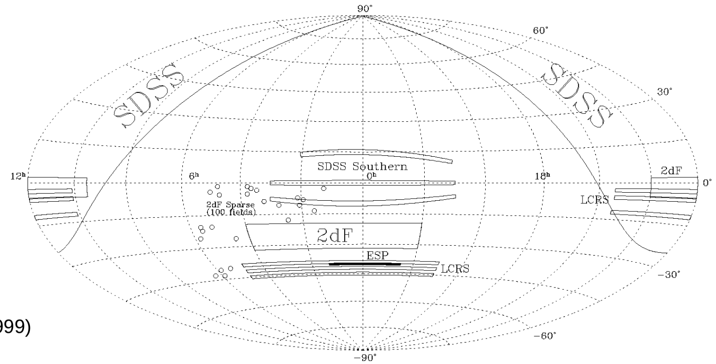

(Strauss, 1999)

Surveys:

1D-surveys: very deep exposures of small patch of sky, e.g. HST Deep Field, Lockman Hole Survey, Marano Field.

2D-surveys: cover long strip of sky, e.g., CfA-Survey ($1.5 \times 100^\circ$), 2dF-Survey (“2 degree Field”).

3D-surveys: cover part of the sky, e.g., Sloan Digital Sky Survey.

These surveys attempt to go to certain limit in z or m.

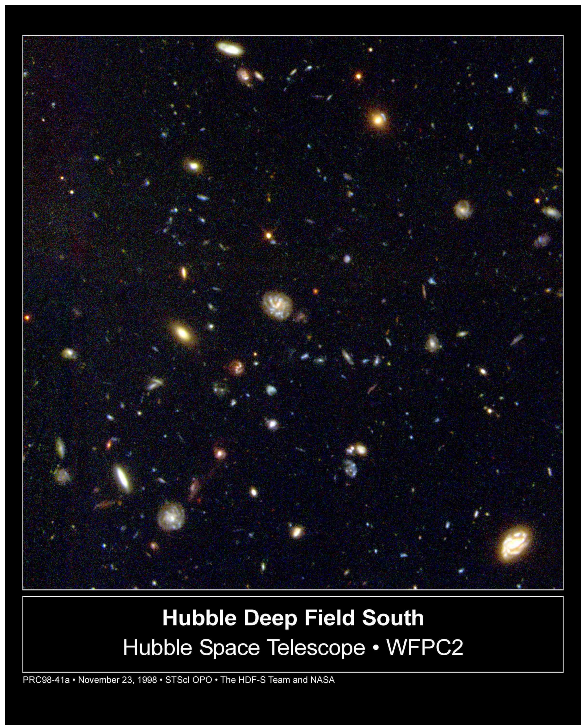

1998: Hubble Deep Field South, 10 d of total observing time!

Spectroscopic surveys, I

Spectroscopic surveys: Identify AGN among other deep-sky objects

Main indicator: strong, broad emission lines

Not found in stars or PNe

Techniques:

- Smith (1975), Osmer & Smith (1975): slitless spectrum technique
  Very efficient for $z > 2$ since it picks up Ly α emission line
- Large survey: Schmidt, Schneider, & Gunn (1986)

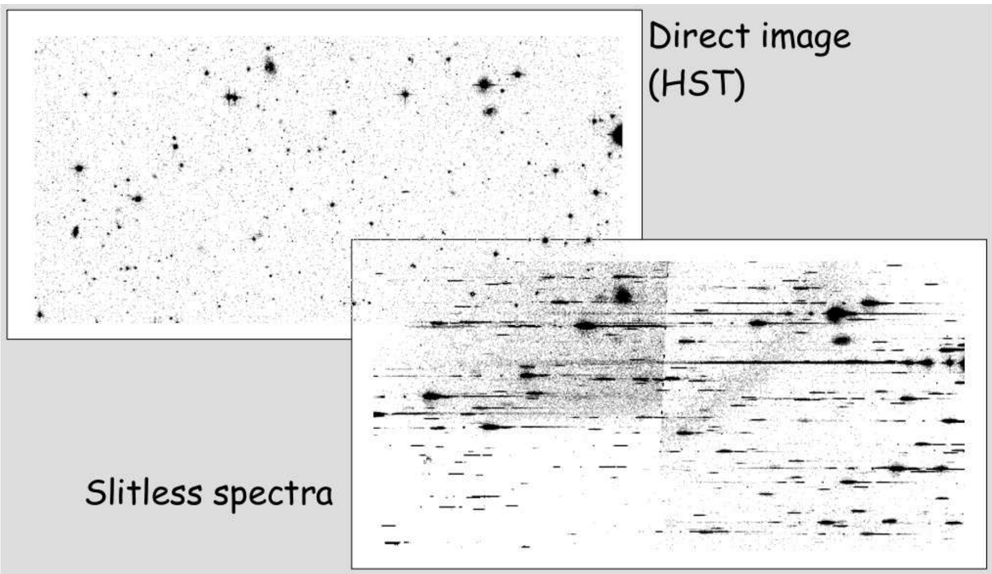

Koopmans, Lecture 10, Slide 15

2D/3D Photometric Surveys

2D and 3D Surveys: observing large part of sky with dedicated instruments.

Currently largest surveys:

Las Campanas Redshift Survey (LCRS): 26418 redshifts in six $1.5 \times 80^\circ$ slices around NGP and SGP, out to $z = 0.2$.

CfA Redshift Survey: 30000 galaxies

APM: (Oxford University) $2 \sim 10^6$ galaxies, 10^7 stars around SGP, 10% of sky, through $B = 21$ mag.

2MASS: IR Survey of complete sky (Mt. Hopkins/CTIO) completed 2000 October 25), 3 bands, $\sim 2 \times 10^6$ galaxies, accompanying redshift survey (8dF, CfA)

Sloan Digital Sky Survey (SDSS): dedicated 2000 October 5, Apache Point Obs., NM, 25% of whole sky, $\sim 10^8$ objects, now in Google Earth

Plans: PanSTARRS, LSST

SDSS 2.5 m telescope at Apache Point Observatory

courtesy SDSS

2D/3D Photometric Surveys

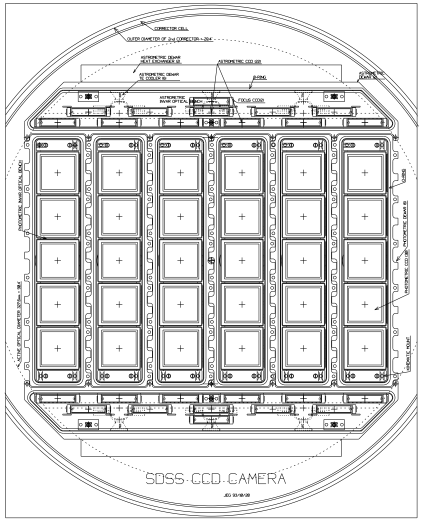

CCD alignment of SDSS:

- focal plane: 2.5°,
- 5 rows of 2048 × 2048 CCDs with r, i, u, z, g filters, saturation at $r = 14$
- 22 2048 × 400 CCD, saturation at $r = 6.6$ for astrometry

Imaging by slewing over CCD Array

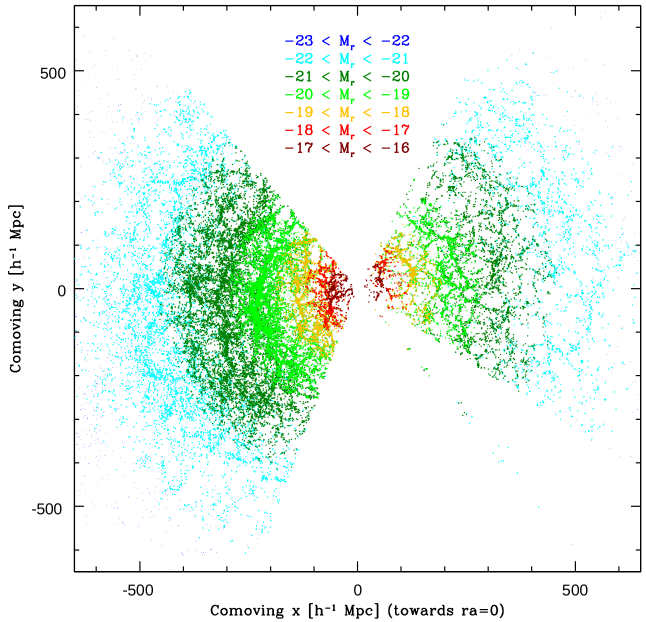

Galaxy distribution from the SDSS

(Tegmark et al., 2004, Fig. 4)

2D/3D Photometric Surveys

courtesy SDSS

Spectroscopy with grism (combination of prism and grating), light from objects via optical fibers and plug plate.

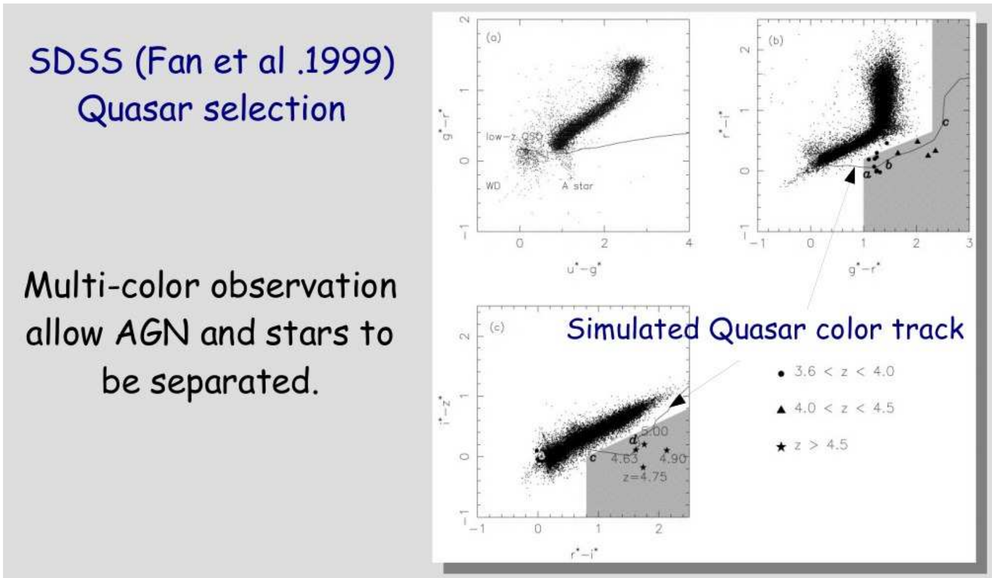

Koopmans, Lecture 10, Slide 17

At very high redshifts, contamination with L dwarfs (very low-mass stars) might become a problem (Fan et al. 2001)

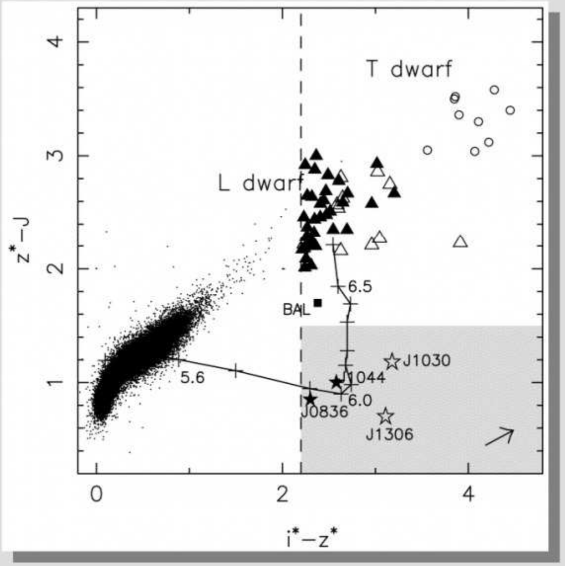

Koopmans, Lecture 10, Slide 18

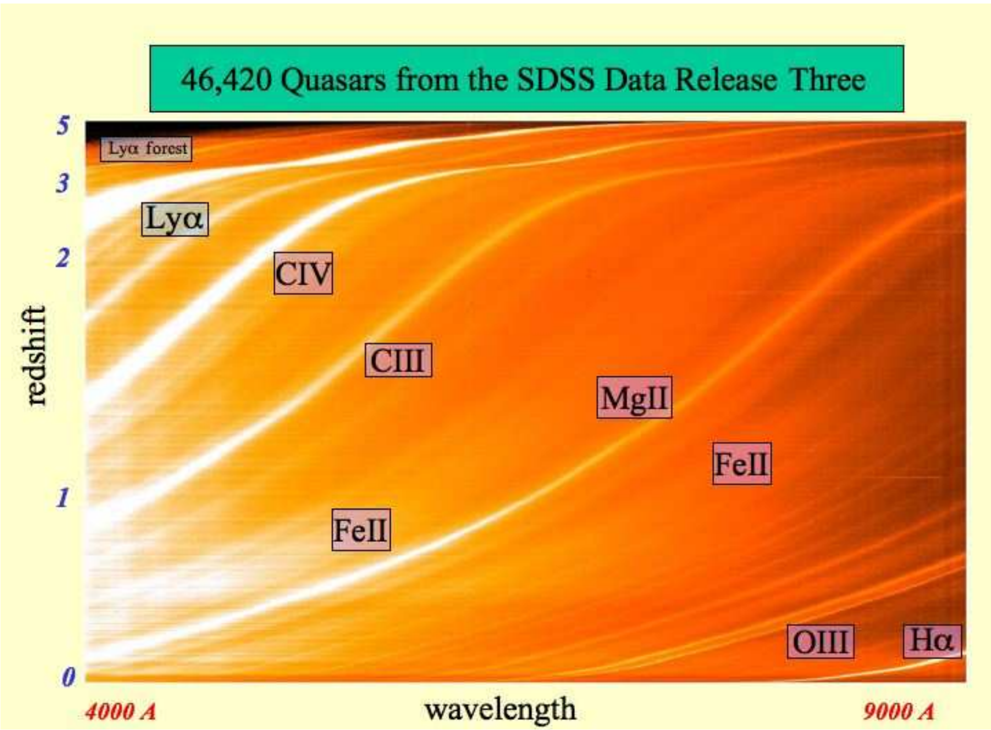

2D/3D Photometric Surveys

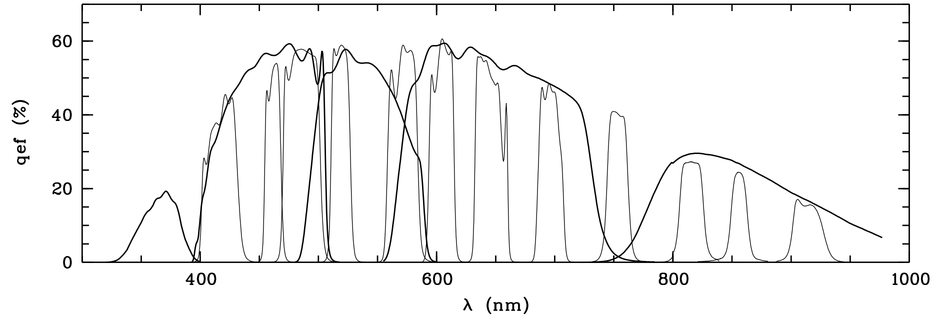

(COMBO-17 survey Wolf et al., 2003)

We can use the change of the spectral shape with z to measure photometric redshifts

(necessary to study evolution)

Deep X-ray Surveys


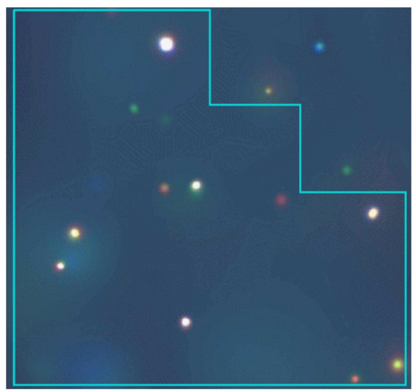

Chandra/HST Image of Hubble Deep Field North; 500 ksec

Problem of optical surveys: many sources are not AGN

Joint multi-wavelength campaigns allow the measurement of broad-band spectra of sources in the early universe!

Deep X-ray Surveys

Deep optical surveys: Many foreground objects

$\Longrightarrow$ go into the X-rays, where AGN dominate

$\Longrightarrow$ Deep X-ray Surveys

Review: Brandt & Hasinger (2005)

History:

- Early 1970s: *Uhuru* and *Ariel*: strong cosmic X-ray background (CXRB)
- Early 1980s: *Einstein* satellite (Wolter telescope): 25% of the 1–3% CXRB resolved into discrete sources, mainly AGN
  Sensitivity limit: $3 \times 10^{-14}\,\mathrm{erg\,cm^{-2}\,s^{-1}}$
- Early 1990s: *ROSAT* resolves ~75% of CXRB into discrete sources
  Sensitivity limit: $10^{-15}\,\mathrm{erg\,cm^{-2}\,s^{-1}}$, AGN density: 780–870 per square degree
- Late 1990s: surveys with *ASCA* and *BeppoSAX*
- State of the art: Chandra and *XMM-Newton* Deep Fields.

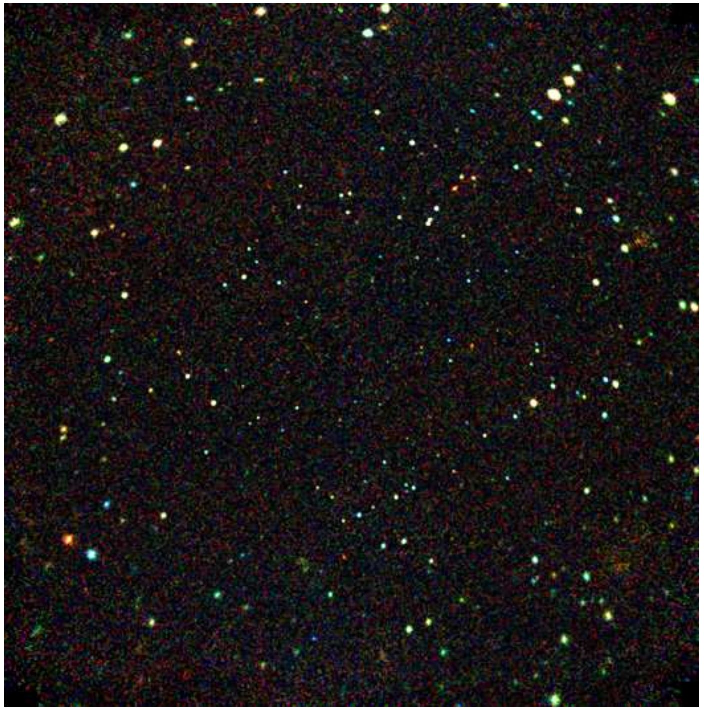

Chandra Deep Field South: 1 Msec (10.8 days) on one region in Fornax
$\Longrightarrow$ Deepest X-ray field ever...

color code: spectral hardness

$\gtrsim 70\%$ of sources in deep X-ray surveys are AGN
in deepest *Chandra* fields, AGN density is $\approx 7200\,\mathrm{deg}^{-2}$ (Bauer et al., 2004)
scale: $15' \times 15'$; courtesy NASA/JHU/AUI/R.Giacconi et al.

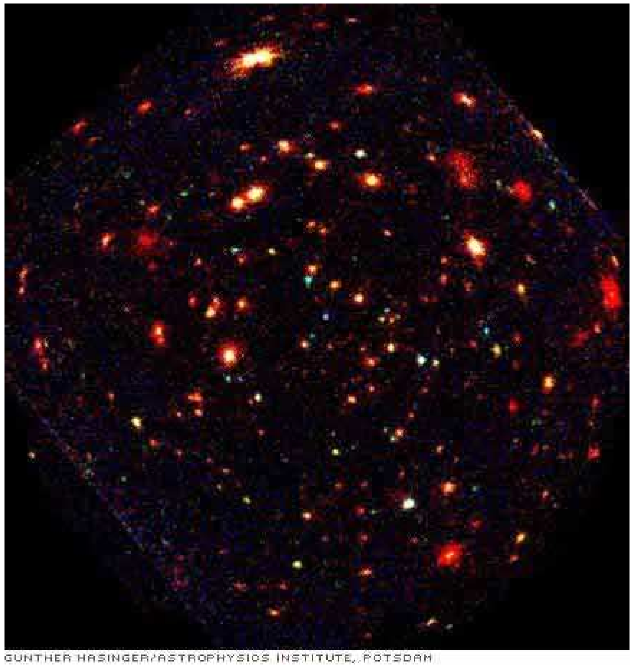

Lockman Hole: Northern Sky region with very low N_H
$\Longrightarrow$ low interstellar absorption
$\Longrightarrow$ "Window in the sky"
$\Longrightarrow$ X-rays: evolution of active galaxies with z!
XMM-Newton, Hasinger et al., 2001,
blue: hard X-ray spectrum,
red: soft X-ray spectrum

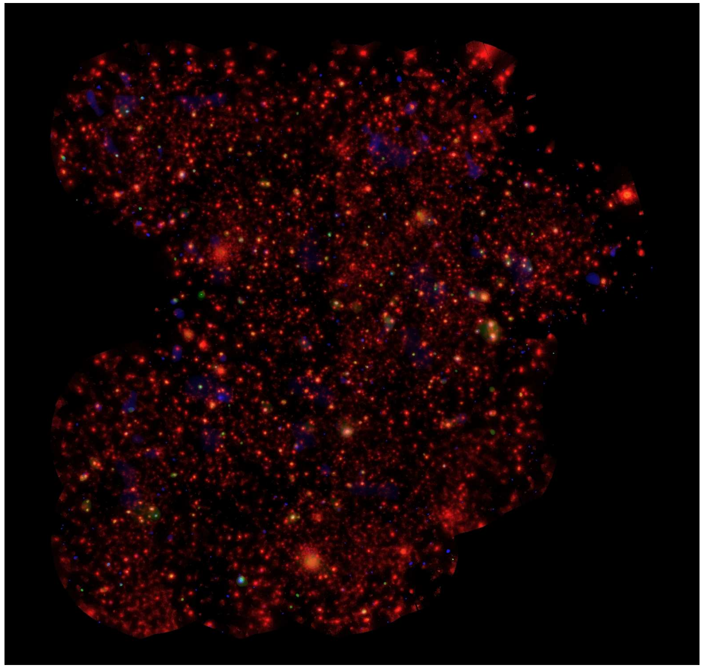

COSMOS field: 1.4 Msec (16.4 days) with *XMM-Newton*, observations from the IR to the X-rays are available

color code: spectral hardness

682 sources detected

courtesy MPE

AGN Statistics

AGN Statistics:

We want to understand how AGN develop in time

$\Longrightarrow$ perform AGN surveys according to well understood criteria:

- Redshift limited samples
- Luminosity limited samples

To understand results from surveys, we need to look at the AGN statistics first.

Statistics, I

Most important statistics: number counts

Assume AGN have a space density $n(r)$ as a function of distance.

To illustrate, first look at the number of objects of same luminosity, L, ("δ-function luminosity function") in an Euclidean space:

$$\mathrm{d}N(r) = n(r)\mathrm{d}V = n(r)r^2\mathrm{d}r\mathrm{d}\Omega \tag{11.1}$$

such that surface density (AGN at distance r per square degree):

$$\frac{\mathrm{d}N(r)}{\mathrm{d}\Omega} = n(r)r^2\mathrm{d}r \tag{11.2}$$

Often: flux limited sample: count all sources with $F > S$, i.e., out to distance

$$r_{\max} = \left(\frac{L}{4\pi S}\right)^{1/2} \tag{11.3}$$

Number of sources detected:

$$N(>S) = \int_0^{r_{\max}} n(r)r^2\mathrm{d}r \tag{11.4}$$

cumulative source distribution as a function of flux

Statistics, II

As an example, let's calculate $N(>S)$ for an uniform space density, $n(r) = n_0$:

$$N(>S) = \int_0^{r_{\max}} n(r)r^2\mathrm{d}r = \int_0^{r_{\max}} n_0 r^2\mathrm{d}r = \frac{n_0 r_{\max}^3}{3} = \frac{n_0}{3}\left(\frac{L}{4\pi S}\right)^{3/2} \tag{11.5}$$

or

$$\log(N(>S)) = \log\left(\frac{n_0 L^{3/2}}{3(4\pi)^{3/2}}\right) - \frac{3}{2}\log S \tag{11.6}$$

For a constant source population, the slope in a $\log N$–$\log S$ diagram is $-3/2$.

Disregarding cosmological effects.

When working in magnitudes: $m \propto -2.5\log S \Longrightarrow \log S \propto -0.4m$, such that

$$\log N(m) \propto 0.6m \tag{11.7}$$

So for a constant space density, number of objects detected increases by a factor $10^{0.6} = 4$ per optical magnitude.

In an optical flux limited sample, 80% of all sources are within 1 mag of the detection limit...

Statistics, III

The slope of the $\log N(>\ S)$–$\log S$-relationship for constant density and δ-function luminosity function is

$$\beta = -\frac{\mathrm{d}\log N}{\mathrm{d}\log S} = \frac{3}{2} \tag{11.8}$$

Now include cosmology. Again, for sources with a δ-function luminosity function (=one-to-one relation between flux and redshift), β can be written

$$\beta = -\frac{\mathrm{d}\log N}{\mathrm{d}\log S} = -\frac{\mathrm{d}\log V}{\mathrm{d}\log z}\cdot\frac{\mathrm{d}\log z}{\mathrm{d}\log S} \tag{11.9}$$

For $\Omega = 1$ and $z \gg 1$, Peacock (1999) shows:

$$\frac{\mathrm{d}\log V}{\mathrm{d}\log z} \sim \frac{1.5}{\sqrt{z}} \quad \text{and} \quad \frac{\mathrm{d}\log S}{\mathrm{d}\log z} \sim -(1+\alpha) \tag{11.10}$$

for power law source spectra, $F_\nu \propto \nu^{-\alpha}$, such that

$$\beta = \frac{3}{2}\cdot\frac{1}{(1+\alpha)\sqrt{z}} < \frac{3}{2} \tag{11.11}$$

The problem: Measurements show $\beta \gtrsim 1.5$, i.e., AGN population is evolving.

Biases

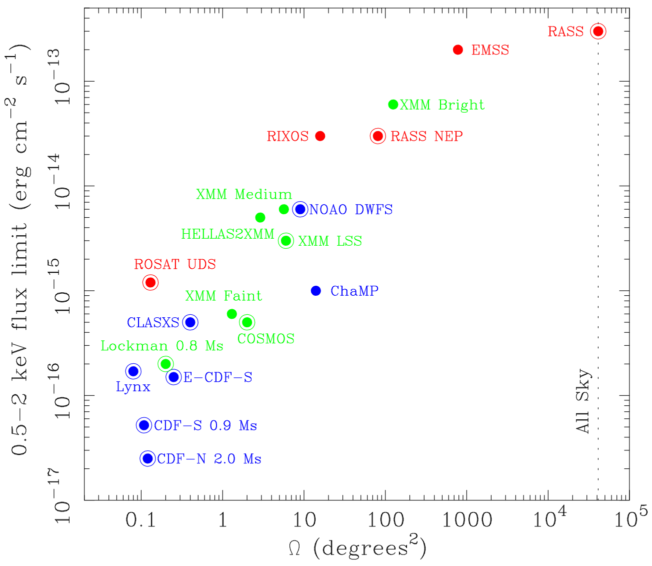

Sensitivity limits of the most prominent X-ray AGN surveys.

Brandt & Hasinger (2005, Fig. 1)

Biases

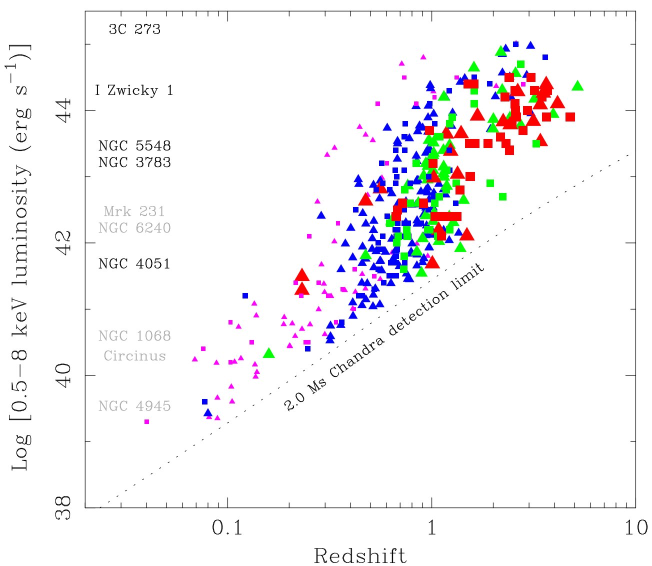

Distant AGN have to be very luminous to be detectable!

Brandt & Hasinger (2005, Fig. 3)

Biases

Flux-limited samples are biased:

- Eddington bias: because of noise, observed number is convolved with noise "point spread function"
- Variability: sources change their brightness $\Longrightarrow$ not complete!
- Absorption lines: for high z, absorption in intergalactic medium changes spectra
- Internal absorption: dependence of viewing angle, dust in host galaxy (looking for type II AGN is more difficult)

AGN Evolution: Observations, I

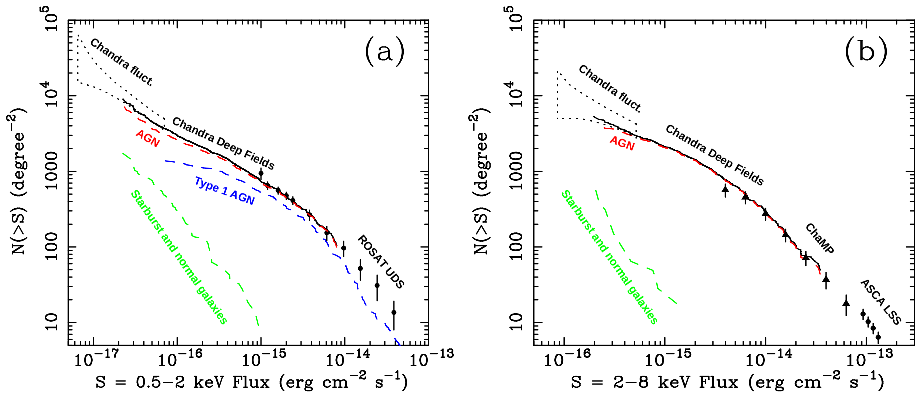

Brandt & Hasinger (2005, Fig. 3)

Contributions of different identified types of AGN to total $\log N$–$\log S$: AGN dominate

AGN Evolution: Observations, II

Surveys show that the local distribution of AGN can be parameterized as

$$\rho(L) = \rho_0 \left[\left(\frac{L}{L^*}\right)^{\alpha} + \left(\frac{L}{L^*}\right)^{\beta} \right]^{-1} \quad (11.12)$$

with $\alpha = 0.3$, $\beta = 2.3$, $\rho_0 = 10^{3.6} h^{-3}\,\mathrm{Gpc}^{-3}$ and $L^*_{0.5-2\,\mathrm{keV}} = 10^{42.8}\,\mathrm{erg\,s^{-1}}$ for $z = 0$. At $z \sim 2$: L^* factor 30 larger, find $L \propto (1+z)^3 \Longrightarrow$ AGN Evolution!

General Ansatz: parameterize AGN density, ρ, as function of emitted power L and redshift, z. Two extreme cases

$$\rho(L,z) = \begin{cases} f(z)\rho_0(L) & \text{pure density evolution} \\ \rho_0(L/g(z)) & \text{pure luminosity evolution} \end{cases} \quad (11.13)$$

the evolution functions $f(z)$ and $g(z)$ are often parameterized as powers of $1+z$.

AGN Evolution: Observations, III

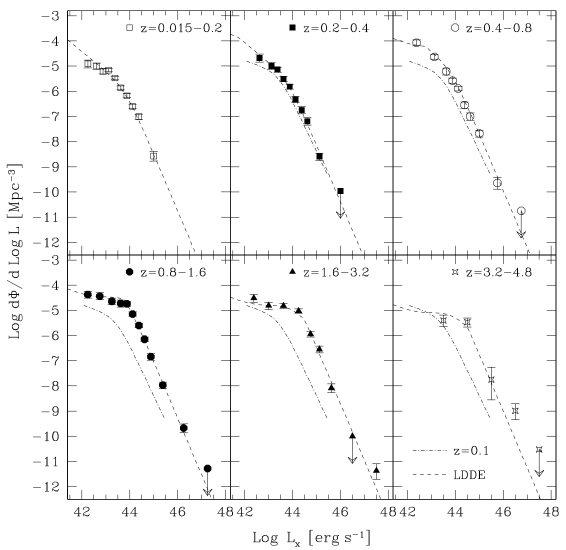

Evolution of $\log N$–$\log S$-with redshift: changes at high L_X!

(Brandt & Hasinger, 2005, Fig. 7)

Observed Space Density

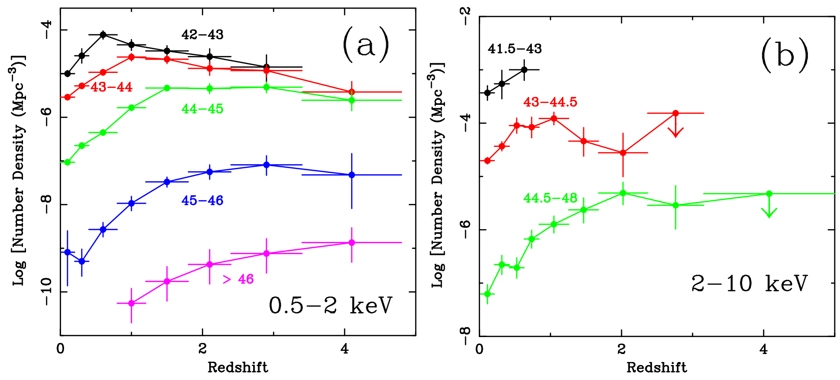

Brandt & Hasinger (comoving AGN space density; 2005, Fig. 8)

X-ray surveys show luminosity evolution:

- peak space density moves to smaller z with smaller L_X
- rate of evolution from now to peak is slower for less luminous AGN: less evolution for low L_X.

$\Longrightarrow$ if L_X traces M_{BH}, then the most massive BH formed first! (“anti-hierarchical AGN evolution”)

Observed Space Density

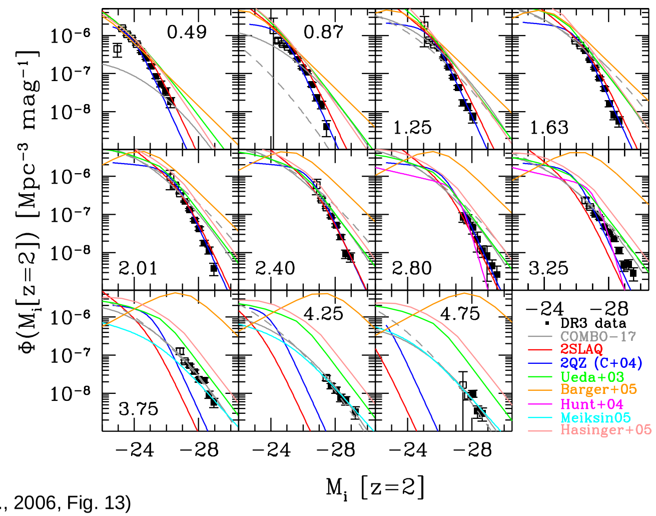

(Richards et al., 2006, Fig. 13)

X-ray fields too small to cover high luminosity quasars $\Longrightarrow$ optical surveys

Observed Space Density

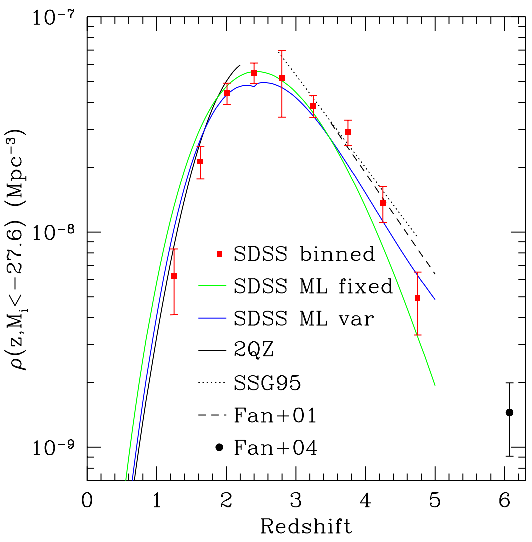

Optical surveys such as the Sloan Digital Sky Survey (SDSS) also show quasars to peak at $z \sim 2$.

(Richards et al., 2006, Fig. 20)

Observed Space Density

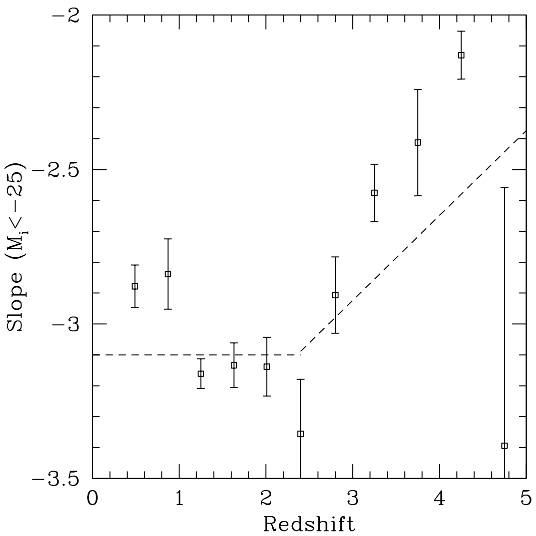

SDSS also shows strong quasar evolution, mainly density evolution, but similarly to X-rays data start to hint also at luminosity dependent density evolution.

(Evolution of luminosity function slope, $\Phi \propto L^{-\beta}$, Fig. 21 of Richards et al., 2006)

AGN and Host Galaxies

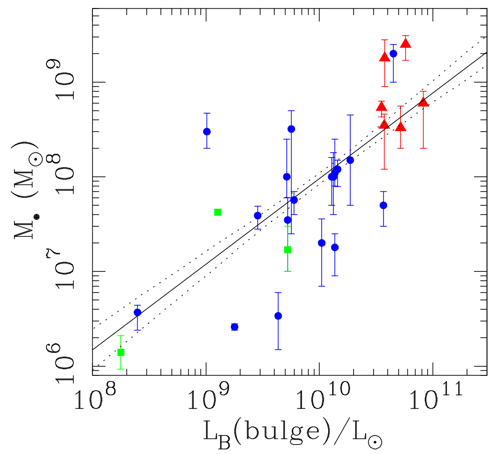

Evolution models predict large numbers of dormant BH in local galaxies. These are indeed found:

The BH mass scales with the luminosity of host galaxy bulge.

See (Ferrarese & Ford, 2005) for a review.

(Gebhardt et al., 2000, Fig. 2)

$$\log(M_\bullet) = (8.37 \pm 0.11) - (0.419 \pm 0.085)(B_T^0 + 20.0) \quad (11.14)$$

AGN and Host Galaxies

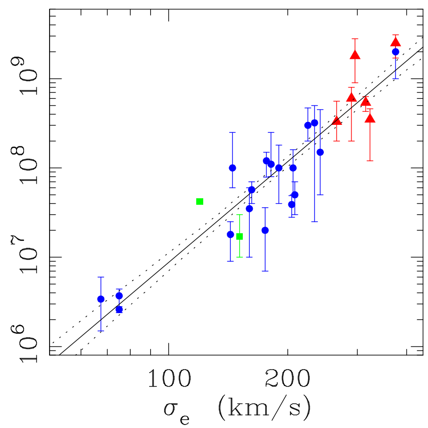

The BH mass scales with the velocity dispersion of the host galaxy bulge.

See Ferrarese & Ford (2005) for a review.

Consequence: Black Hole formation and bulge formation are closely related to each other

Even though AGN exist in bulge-less galaxies.

(Gebhardt et al., 2000, Fig. 2)

$$\frac{M_\bullet}{10^8 M_\odot} = (1.66 \pm 0.24)\left(\frac{\sigma}{200\,\mathrm{km\,s^{-1}}}\right)^{4.86\pm0.43} \text{ to } \sim 30\% \quad (11.15)$$

Quasar Intrinsic Spectral Properties

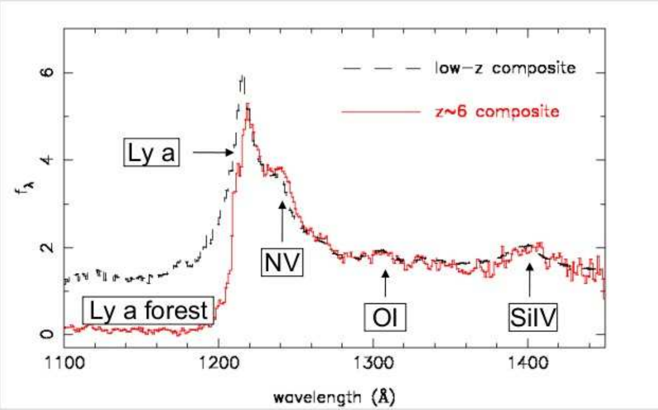

- Rapid chemical enrichment in quasar vicinity
- Quasar env has supersolar metallicity -- metal lines, CO, dust etc.
- High-z quasars and their environments mature early on

Koopmans, Lecture 10, Slide 38

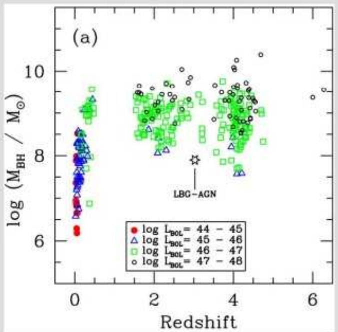

Vestergaard 2004

Formation timescale (assuming Eddington)

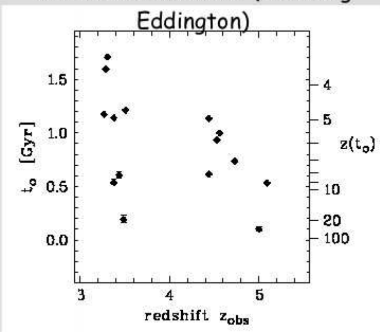

Dietrich and Hamann 2004

Lack of spectral evolution in high-redshift quasars -> quasar BH estimate valid at high-z

BH mass estimate: using emission line width to approximate gravitational velocity, accurate to a factor of 3 - 5 locally

Billion solar mass BH at z~6 indicates very early growth of BHs in the Universe

Koopmans, Lecture 10, Slide 39

AGN Formation

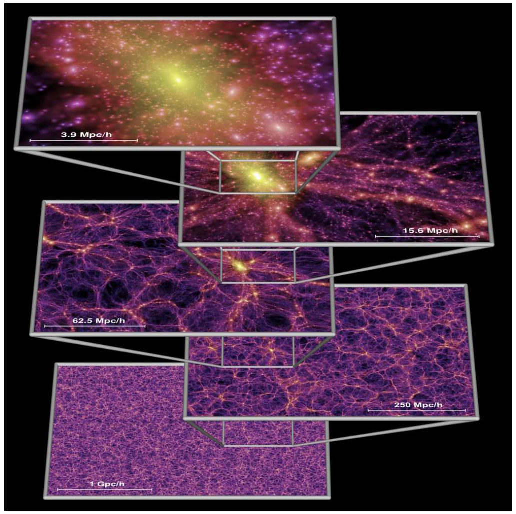

Millenium simulation: numerical simulation of galaxy evolution in a ΛCDM univers, 10$\times$ larger than anything previously done.

Baseline: semi-analytical evolution formalism adjusted to yield galaxy parameters (luminosity-color evolution, morphology, gas content, BH mass) consistent with observations. Covers galaxies down to SMC size, includes AGN formation and growth.

See Springel et al. (2005) for details.

AGN Formation

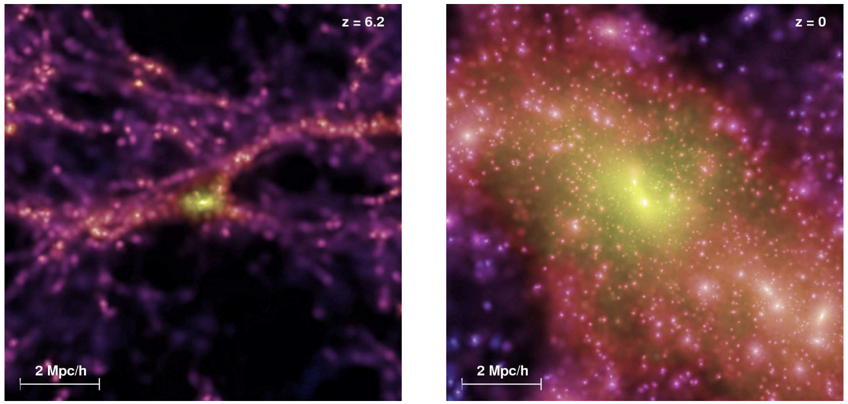

(Springel et al., 2005)

Volume of Millenium simulation too small to contain more than a few quasar candidates.

Here: Evolution of largest mass object, from halo dark matter mass 1.8 $\times$ 10^{10} $M_\odot$ at z = 16.7 to now 3.9 $\times$ 10^{12} $M_\odot$ in DM, 6.8 $\times$ 10^{10} $M_\odot$ normal matter, and a star formation rate of 235 $M_\odot$ year^{-1}.

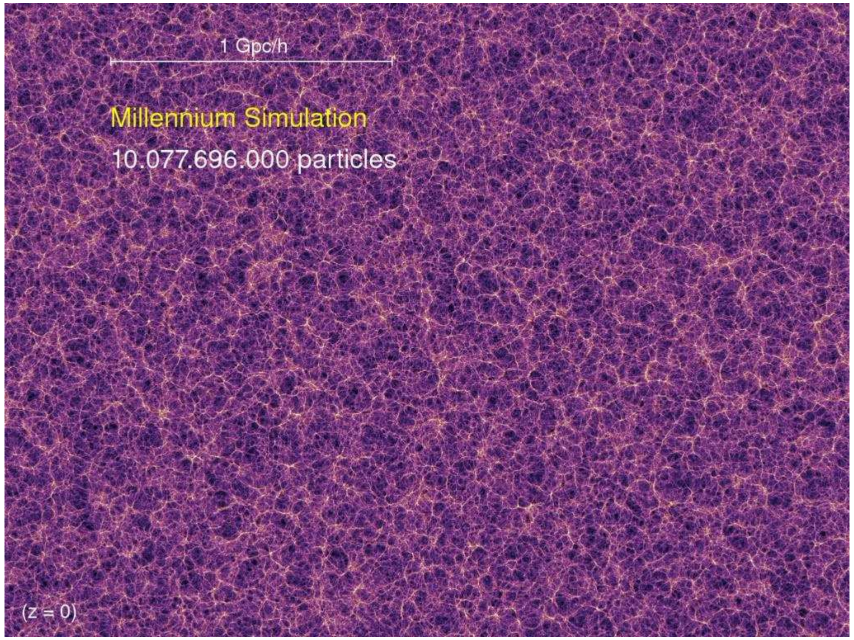

Movie Time: The Millenium Simulation, `formationmovies/millennium_sim_1024x768.avi`
(10^{10} particles; 512 processors, 350000 h (28 clock days) of CPU time, see Springel et al. 2005)

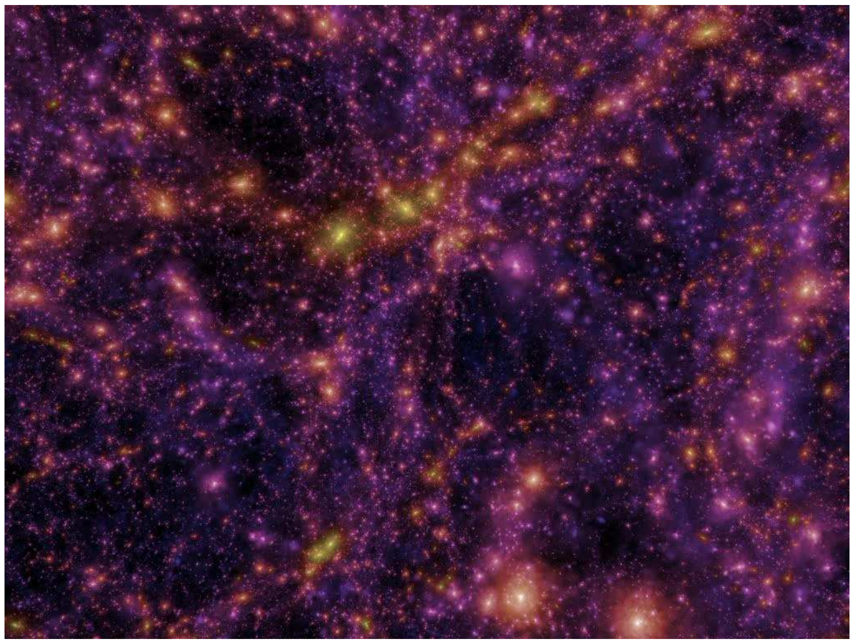

Movie Time: Fly through the Millenium Simulation, `formationmovies/millennium_flythru.avi`
2.5 billion light years; see Springel et al. 2005

AGN Formation

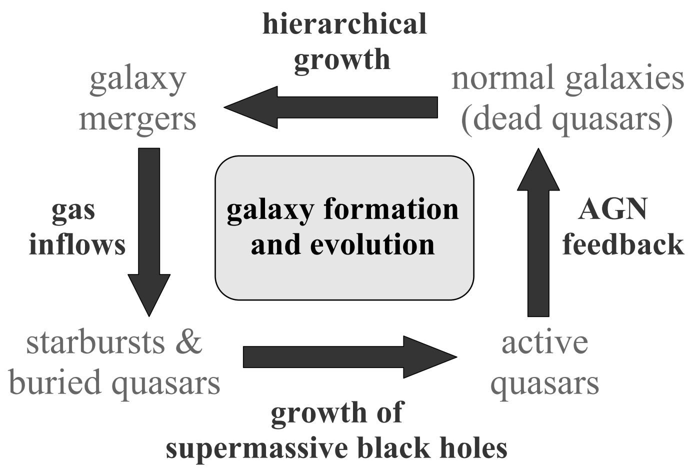

(Hopkins et al., 2006, Fig. 1)

AGN formation and evolution are probably linked to galaxy mergers.

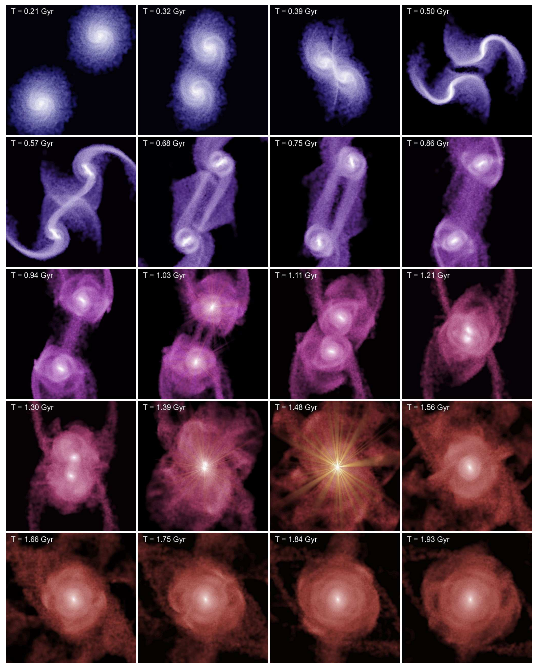

Evolution of a merger in a $80h^{-1}$ kpc wide box: blue: baryonic mass fraction 20%, red: $< 5\%$.
Point sources shown when quasar activity would be observable.

(Hopkins et al., 2006, Fig. 2)

Bauer, F. E., Alexander, D. M., Brandt, W. N., Schneider, D. P., Treister, E., Hornschemeier, A. E., & Garmire, G. P., 2004, AJ, 128, 2048

Brandt, W. N., & Hasinger, G., 2005, Ann. Rev. Astron. Astrophys., 43, 827

Ferrarese, L., & Ford, H., 2005, Space Sci. Rev., 116, 523

Gebhardt, K., et al., 2000, ApJ, 539, L13, erratum: ApJ 555, L75

Hopkins, P. F., Hernquist, L., Cox, T. J., Di Matteo, T., Robertson, B., & Springel, V., 2006, ApJS, 163, 1

Peacock, J. A., 1999, Cosmological Physics, (Cambridge: Cambridge Univ. Press)

Richards, G. T., et al., 2006, AJ, 131, 2766

Springel, V., et al., 2005, Nature, 435, 629

Strauss, M. A., 1999, in Structure Formation in the Universe, ed. A. Dekel, J. P. Ostriker, (Cambridge: Cambridge Univ. Press)

Tegmark, M., et al., 2004, ApJ, 606, 702

Wolf, C., Meisenheimer, K., Rix, H., Borch, A., Dye, S., & Kleinheinrich, M., 2003, A&A, 401, 73